

Preliminary design of centrifugal compressor using multidisciplinary optimization method

Sun Shouyi, Yue Zhufeng, Li Lei*, Zhang Mengchuang, and Yang Weizhu

Department of Engineering Mechanics, Northwestern Polytechnical University (Chang'an Campus), P.O. BOX 16m, Xi'an 710129, PR China

Received: 27 February 2018 / Accepted: 4 October 2019

Abstract. Centrifugal compressor is widely used in turbochargers in which the aerodynamic performance and strength are invariable among the important design objectives. As high pressure ratio centrifugal compressor develops, the interaction between multiple disciplines should be involved in the preliminary design process. A strength prediction method was presented and the prediction error was less than 3% compared with the 3D finite element calculation. The preliminary design method was established with consideration of multidisciplinary couplings. Then, a centrifugal compressor with the lowest pressure ratio of 4.4 was designed based on the method. The optimal results showed that the aerodynamic efficiency increases by 2.245% compared with the initial design results. Finally, the 3D validation was carried out including aerodynamic analysis and strength calculation, which showed good agreement with the optimal results of the preliminary design.

Keywords: Centrifugal compressor / performance prediction / strength prediction / multidisciplinary optimization / preliminary design

1 Introduction

Centrifugal compressor is widely used in turbochargers because of its high reliability, simple structure, high single stage pressure ratio and other prominent characteristics. At present, the preliminary design still acts as an important role in the entire design flow, it determines whether the centrifugal compressor design is successful or not [1]. Furthermore, the basic geometric parameters of the centrifugal compressor are mainly obtained by one-dimensional (1D) calculations and analysis during the preliminary design process [2]. Hence, to get a well-designed centrifugal compressor with high performance, the accurate aero-thermodynamic and structural analysis should be involved in the preliminary design process.

In the preliminary design process, the aerodynamic performance prediction should be conducted at both design and off-design points [3]. Although the computational fluid dynamics has been impressively developed, it increases the time cost. Therefore, the conventional mean-line method using empirical loss models is still the most practical way to predict the off-design performance of the centrifugal compressor [4,5]. In the past few years, 1D aerodynamic performance analysis method has been developed persistently. Oh et al. presented a reliable performance

prediction method of centrifugal compressor considering various empirical loss models, which agreed fairly well with experimental data for a variety of centrifugal compressors [5]. Galvas analyzed the off-design performance of centrifugal compressor with the introduced 1D model by considering surge and choke margins [6]. Muralidharan presented a 1D analysis method and achieved the design of a centrifugal compressor, of which the total to total pressure ratio was up to 8 [2]. Aungier proposed a comprehensive mean streamline performance analysis method for centrifugal compressor stage, and the detailed validation was reliable against experimental data [7]. Li used a new optimum set of loss models to predict the performance of a low pressure stage centrifugal compressor, the results showed good agreements with the experimental data [1]. On the whole, 1D aerodynamic performance analysis method is time saving compared with three-dimensional (3D) fluid analysis.

As high pressure ratio centrifugal compressor develops, the blade is becoming thinner and over-backswept. Besides, increased impeller rotation speed, outlet temperature and aerodynamic force will promote impeller failure [8]. Xu analyzed the high-stress locations of the centrifugal compressor impeller by using finite element method, he found that the impeller was easy to fail at the root of the leading edge area [9]. Lerche and Kang used a fluid-structure interaction (FSI) model to predict stress of centrifugal compressor blade, in which pressures were

* e-mail: lileinpu@nwpu.edu.cn

transferred to the structural codes unidirectionally [10,11]. In general, strength checks are often carried out during the detailed design process. However, fewer studies about 1D strength prediction method are conducted. When the mechanical requirements are not satisfied, the centrifugal compressor would be redesigned which is time consuming.

Centrifugal compressor is a complicated system that is subjected to multidisciplinary coupling and should meet multi-objective requirements. Hence, the multidisciplinary design optimization (MDO) method is frequently used to improve accuracy of the compressor design. At present, there are many multidisciplinary coupling methods to solve the MDO problem, including Multi-Disciplinary Feasible Design (MDF), Individual Discipline Feasible (IDF), Collaborative Optimization (CO), Concurrent Subspace Optimization (CSSO), and Bi-Level Integrated Synthesis System (BLISS), etc. [12]. And the MDF method was preferred for its convenience of implementation. Yu optimized the blade profile of a centrifugal compressor by applying the MDF method [13]. Zhang presented a reliability-based multidisciplinary design optimization frame work for centrifugal compressor to design blade [14]. However, the multidisciplinary optimization process of centrifugal compressor is mostly carried out in the detailed design process rather than in the preliminary design process.

This paper presents a preliminary design method for the centrifugal compressor based on multidisciplinary optimization. First, a performance prediction method is introduced by considering various loss models. Second, a strength prediction method is proposed to analyze the stress state around the hub of compressor leading edge. Third, the basic structural parameters are optimized considering multiple objectives and multiple disciplines. Final, the optimal results are verified by the 3D aerodynamic analysis and structural finite element analysis.

2 Preliminary design method considering multidisciplinary coupling

2.1 The structure of MDO system

The MDO method is used to achieve the best design under the joint action of multiple interacting disciplines. Normally, each disciplinary in a n disciplines coupling system is described in the following representation:

$$y_i = f(x_i, y_j, z), \quad i, j = 1, \dots, n \quad j \neq i \quad (1)$$

where n is the total number of coupled disciplines, counted by i . y_i represents i th discipline, x_i is the local variables vector. The vector y_j corresponds to interdisciplinary couplings, and z denotes the global or shared variable vector.

As a typical multi-physics model, the design of centrifugal compressor involves aero-thermodynamic and mechanical systems. MDF method is used because of small amounts of design variables. It combines the multidisciplinary design analysis (MDA) with an optimizer to find

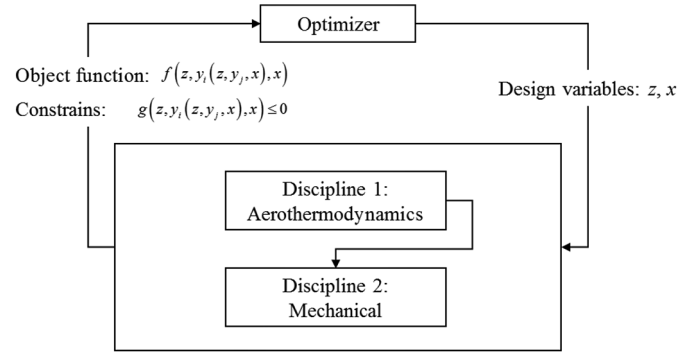


Fig. 1. Framework of MDF.

the optimal solution. The MDF method can be formulated as follows:

$$\begin{cases} \text{find } x \\ \min f(z, y_i(z, y_j, x), x) \quad i, j = 1, \dots, n \quad j \neq i \\ \text{s.t. } g(z, y_i(z, y_j, x), x) \leq 0 \\ x^l \leq x \leq x^u \end{cases} \quad (2)$$

where f is the objective function and g represent all the equality and inequality system constraints. x , x^l and x^u are vectors of design variables, variable lower bounds and upper bounds, respectively. z is design parameters. The framework is shown in Figure 1.

2.2 Preliminary design and analysis method

The 1D aero-thermodynamic calculation is an approximate method to solve the complicated flow inside impeller machinery. It is assumed that the internal flow is one-dimensional, which means the physical fluid parameters perpendicular to the direction of flow are equal, while variable in other directions. The preliminary design of centrifugal compressor is an iterative process, and the detailed calculation process is described below.

2.2.1 1D calculation

2.2.1.1 Impeller inlet

The goal of centrifugal compressor inlet design is to get the minimum inlet relative Mach number at shroud ($W_{1,s}$) for a given mass flow and structural requirements. The difference of mass flow between choke and stall is significantly reduced with an unreasonable inlet relative Mach number, which will lead to a bad operation range. For a given inlet conditions, there exists a unique absolute inlet velocity that satisfies the minimum inlet Mach number. Therefore, it is an optimization process for the centrifugal compressor impeller inlet design. The nonlinear programming method is used to solve the optimization problem. As the inlet design begins, the pressure ratio (π_i), work fluid properties, the inlet total pressure (P_0), total temperature (T_0) as well as the mass flow (\dot{m}) must be known. Besides, the following data should be determined based on the design experience: the impeller rotational speed (n), blockage factor (B),

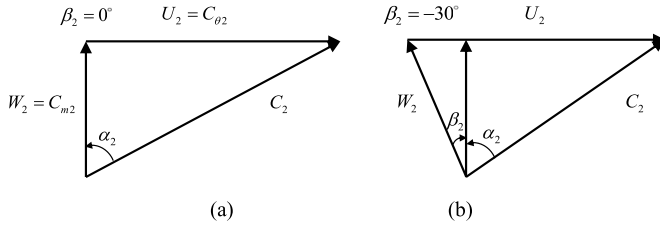


Fig. 2. Triangle of velocities.

hub-shroud radius ratio (r_{1h}/r_{1s}) or the hub radius (r_{1h}). The r_{1h}/r_{1s} is general range from 0.3 to 0.5. A greater one will lead to impeller premature blockage because of reduced inlet flow area, while the inlet Mach number of impeller shroud will be too big for a smaller r_{1h}/r_{1s} . The goal of inlet design is to get a minimum W_{1s} and corresponding design values of impeller inlet.

2.2.1.2 Impeller outlet

The impeller outlet flow angle, blade height and the impeller diameter are concluded from the impeller outlet design. According to the 1D steady flow equations, the relationship between the impeller pressure ratio and impeller inlet and outlet velocity is as shown in equation (3)

$$\left(\frac{P_{02}}{P_{01}}\right)^{\frac{k-1}{k}} = 1 + \frac{k-1}{kRT_{01}} \eta_l (U_2 C_{\theta 2} - U_1 C_{\theta 1}). \quad (3)$$

The impeller pressure ratio is only related to the outlet parameters and impeller efficiency if the inlet flow direction is axial. The back sweep angle (β_2) is of great benefit to improve compressor performance. Figure 2 shows the triangle of velocities of two types impeller with two different back sweep angle of 0° and -30° , which are corresponding to radial impeller and backswept impeller, respectively.

When the total work of the radial impeller and backswept impeller is equal, i.e. they have the same $U_2 C_{\theta 2}$, the absolute flow angle of the backswept impeller exit is smaller than that of radial impeller. The velocity at impeller exit decreases as the back sweep angle increases, which will lead to a wide surge margin. However, a bigger back sweep angle would give rise to the stress levels [15]. Besides, the back sweep angle increases the radius of curvature of streamline at S1 stream surface. The centrifugal force of the blade would counteract the pressure difference between pressure side and suction side, and further reducing the flow loss of the secondary flow. Hence, an appropriate design of back sweep angle is the key to high performance centrifugal compressor.

In order to reflect the phenomenon of jet-wake, the slip factor is used to model the flow deviation and calculate the tangential absolute velocity component at the impeller outlet. Stanitz [16], Weisner [17], Qiu [18] have proposed many different forms of the model, and Weisner slip factor is frequently used for its good correlation with a lot of

experiments:

$$\mu = 1 - \sqrt{\cos \beta_2} / Z^{0.7}. \quad (4)$$

The impeller exit absolute flow angle (α_2) is the key parameter which influences both the mixing loss at the impeller exit and the development of the wall boundary layers in the vaneless space. A range of $69^\circ < \alpha_2 < 73^\circ$ is recommended with acceptable mixing loss and vaneless space pressure recovery [15].

2.2.1.3 Diffuser

Diffuser is the device converting kinetic energy into potential energy that fixed on the outlet of centrifugal impeller. The performance of diffuser has an important effect on the aerodynamic efficiency, pressure ratio and stable operation range of centrifugal compressor. And the flow loss of diffuser in the centrifugal compressor is about 30% of the total loss [19,20].

Vaneless diffusers have a wider operating range compared to the vaned diffusers, and there are no fatigue failure problems caused by vibration between blade and impeller. The flow choke phenomenon of diffuser will hardly happen since there is nearly no throat area in vaneless diffuser. But the flow channel length of diffuser should be long enough to get an appropriate diffusing capacity. The long flow channel will increase the friction loss and decrease the aerodynamic efficiency of centrifugal compressor.

2.2.2 Performance prediction

2.2.2.1 Efficiency

According to the mean line approach, a compressor stage can be treated as several characteristic parts, each defined by inlet and outlet surface. Losses occurring in different parts are modeled in the past several decades. The mechanisms of different loss types are various, the corresponding contributions to the entropy increase in turbomachines were described by Whitfield and Denton et al. [21,22]. A poor loss model will cause problems in the design process. Hence, the appropriate loss models of centrifugal compressor should be selected to predict the efficiency of centrifugal compressor accurately.

Furthermore, an optimum loss model set should be chosen during the preliminary design of centrifugal compressor. Recent years, many empirical loss models are available for each respective loss mechanism. Oh [5], Galvas [6], Aungier [7] and others researchers put forward some sets of loss models that agree well with the experimental results. Table 1 presents loss correlations used in the present study.

2.2.2.2 Surge margin

At surge condition, the airflow oscillates at low frequencies throughout the compressor system. Hence, the stage stability is seriously limited by the surge margin. Generally, the backswept angle of centrifugal compressor could lead to a low surge flow and hence larger surge margin, making the locus of peak efficiency away from the surge line [28].

Table 1. Loss correlations.

Loss mechanism	Loss model	Reference
Incidence loss	$\Delta h_{\text{inc}} = 0.4 \left(W_{m1} - \frac{C_{m1}}{\sin \beta_1} \right)^2$	Aungier [7]
Blade loading loss	$\Delta h_{bl} = 0.05 D_f^2 U_2^2$ where: $D_f = 1 - \frac{W_2}{W_{1s}} + \frac{0.75 \Delta h_{\text{Euler}} / U_2^2}{(W_{1s}/W_2)[(Z/\pi)(1 - D_{1s}/D_2) + 2D_{1s}/D_2]}$ $\Delta h_{\text{Euler}} = C_{\theta 2} U_2 - C_{\theta 1} U_1$	Coppage et al. [23]
Skin friction loss	$\Delta h_{sf} = 2C_f \frac{L_B}{D_{\text{hyd}}} \overline{W}^2$ $\overline{W} = \frac{2W_2 + W_{1s} + W_{1h}}{4}$ $L_B = \frac{\pi}{8} \left[D_2 - \frac{D_{1s} + D_{1h}}{2} - b_2 + 2L_z \right] \left(\frac{2}{\frac{\cos \beta_{1s} + \cos \beta_{1h}}{2} + \cos \beta_2} \right)$ $\frac{D_{\text{hyd}}}{D_2} = \frac{\cos \beta_2}{\left[\frac{Z}{\pi} + \frac{d_2 \cos \beta_2}{b_2} \right]} + \frac{\frac{1}{2} \left(\frac{D_{1s}}{D_2} + \frac{D_{1h}}{D_2} \right) \left(\frac{\cos \beta_{1s} + \cos \beta_{1h}}{2} \right)}{\frac{Z}{\pi} + \left(\frac{D_{1s} + D_{1h}}{D_{1s} - D_{1h}} \right) \left(\frac{\cos \beta_{1s} + \cos \beta_{1h}}{2} \right)}$	Jansen [24]
Clearance loss	$\Delta h_{cl} = 0.6 \left(\frac{\Delta n_{cl}}{b_2} \right) \left(\frac{C_{\theta 2}}{U_2} \right) \sqrt{\frac{4\pi}{b_2 Z} \left[\frac{r_{1s}^2 - r_{1h}^2}{(r_2 - r_{1s})(1 + \rho_2/\rho_1)} \right]} \left(\frac{C_{\theta 2}}{U_2} \right) \left(\frac{C_{m2}}{U_2} \right)$	Jansen [24]
Mixing loss	$\Delta h_{\text{mix}} = \frac{1}{1 + \tan^2 \alpha_2} \left(\frac{1 - \varepsilon_{\text{wake}} - b^*}{1 - \varepsilon_{\text{wake}}} \right)^2 \frac{C_2^2}{2}$ where: $\varepsilon_{\text{wake}} = 0.25$, $b^* = 1$	Johnston and Dean [25]
Disc friction loss	$\frac{\Delta h_{df}}{4\dot{m}} = f_{df} \bar{\rho} r_2^2 U_2^3$ where: $\bar{\rho} = \frac{\rho_1 + \rho_2}{2}$ $f_{df} = \begin{cases} \frac{2.67}{Re_{df}^{0.5}}, & Re_{df} < 3 \times 10^5 \\ \frac{0.0622}{Re_{df}^{0.2}}, & Re_{df} \geq 3 \times 10^5 \end{cases}$ $Re_{df} = \frac{U_2 r_2}{\nu_2}$	Daily and Nece [26]
Vaneless diffuser loss	$\Delta h_{vlf} = 2C_{fd} (L_d / D_{\text{hyd}}) C_m^2$ $C_{fd} = k \left(\frac{1.8 \times 10^5}{Re_d} \right)^{0.2}$, $k = 0.015$	Japikse [27]
Recirculation loss	$\Delta h_{rc} = 0.02 D_f^2 U_2^2 \sqrt{\tan \alpha_{2r}}$	Jansen [24]

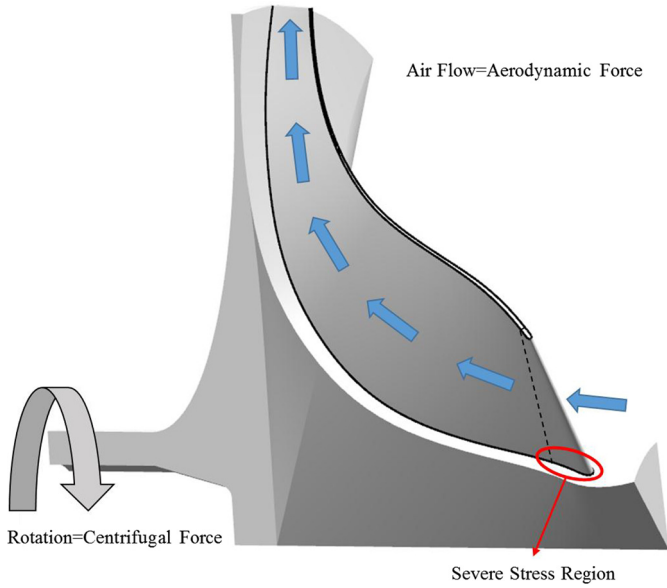


Fig. 3. Impeller topology block structure.

As the number of vanes increases, the distribution of the flow near vanes will be unsteady, which results in a kind of obstruction for the incoming flow to the diffuser [29]. Besides, the diffuser with few vanes contributes to the wide surge margin [30].

The surge point can be defined as the point of maximum total pressure on the compressor characteristic curve. Usually the expression of the surge margin is as follows:

$$SM = \left(\frac{\dot{m}_{\text{design}} - \dot{m}_{\text{surge}}}{\dot{m}_{\text{design}}} \right). \quad (5)$$

2.3 Strength prediction of centrifugal compressor impeller

2.3.1 Strength prediction method

Centrifugal impeller is rotating with the rotor assembly at high rotational speeds. Typically, the tip speed and the material are used to assess structural strength. However, the range of the tip speed is too large to get the precise strength evaluation for the same material [15]. Simultaneously, the high temperature and high speed gas flow through the impeller will affect the stress state of the impeller.

Figure 3 shows a 3D model of a sector of impeller with a single blade. A relatively large stress region is located at the hub of the centrifugal impeller blade near the leading edge, as shown in the red region in Figure 3, which is resulted from the centrifugal force, aerodynamic force and thermal effect.

To calculate the stress state of the impeller blade hub near the leading edge, a strength prediction (SP) method was proposed. The leading edge region of impeller blade before the dotted line in Figure 3 is simplified to an equivalent model, as shown in Figure 4. The root of the

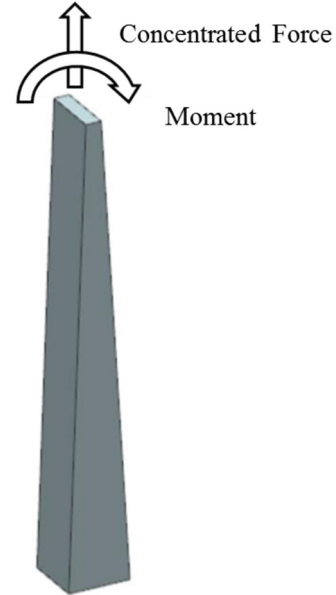


Fig. 4. Equivalent model for strength prediction.

model is a square area with the same width as the blade hub thickness. As the blade thickness gradually decreases along the leading edge from root to tip, the equivalent model is also designed with gradient thickness. A concentrate force is applied on the tip of the equivalent model to simulate the centrifugal force. The moment is to produce bending stress induced by the blade twist, aerodynamic force and thermal effect.

The blade height, flow angle, impeller hub and tip radius, blade thickness can be obtained through the preliminary design. Because the stress at the hub is a superposition of different stress component, which is resulted from different force, the maximum stress at the hub of centrifugal impeller near the leading edge could be described through a linear expression as below:

$$\sigma_{\text{max}} = K_F \sigma_F + K_M \sigma_M \quad (6)$$

where

$$\sigma_F = \frac{1}{t_{1h}^2} \int_{r_{1h}}^{r_{1s}} \rho \Delta V \omega^2 r dr \quad (7)$$

$$\sigma_M = \frac{P_0 t_{1h} (r_{1s} - r_{1h})^2}{2W_b} \quad (8)$$

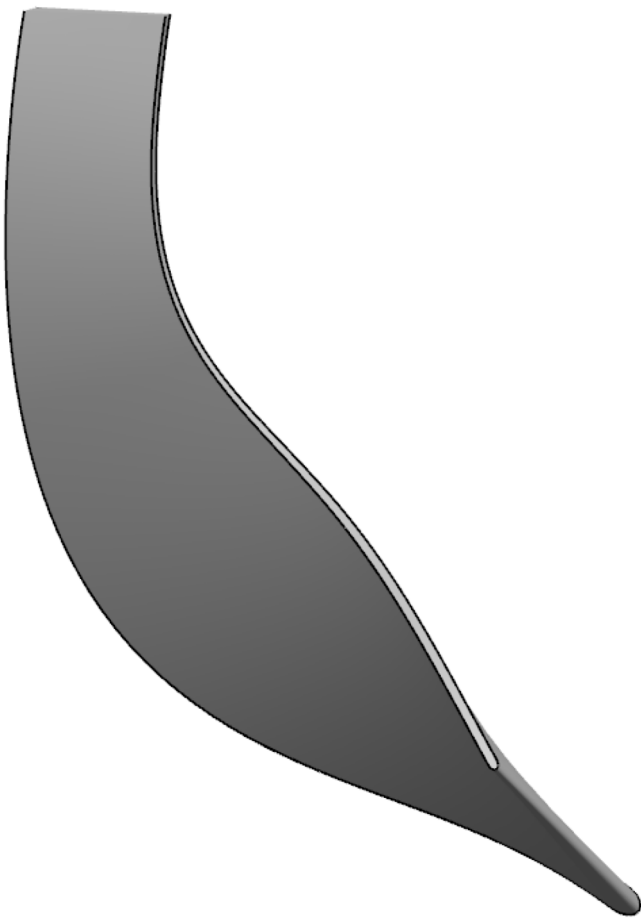
where V represents the volume of the equivalent model. K_F and K_M is the stress coefficient for tensile stress and bending stress, respectively. $W_b = \frac{1}{6} t_{1h}^3$ is the section modulus.

2.3.2 Validation of the strength prediction method

To validate the strength prediction method, the FEM was applied to carry out the mechanical analysis of the impeller blade. The geometric parameters obtained through the 1D aero thermodynamic calculation were used to generate a

Table 2. Comparisons between the FEM and SP.

Num.	π_{design}	ω (rpm)	\dot{m} (kg/s)	Strength prediction (MPa)	Validation of 3D (MPa)	Error
1	5.2	32000	6.0	346.186	345.539	0.187%
2	5.2	28500	6.5	316.811	315.471	0.425%
3	5.2	25000	7.0	281.518	284.435	1.025%
4	5.2	22000	7.5	250.781	244.239	2.678%
5	4.2	28500	6.0	299.889	297.813	0.697%
6	4.2	25000	6.5	265.506	272.541	2.581%
7	4.2	22000	7.0	239.356	239.427	0.030%
8	4.2	20000	7.5	222.617	223.548	0.412%

**Fig. 5.** Geometry of impeller blade.

model of 3D impeller blade is as shown in [Figure 5](#). The hub and shroud profiles were generated by using Bezier curves. Suction surface and pressure surface were modeled through ruled surface in NX 8.0.

The material of the impeller blade was TC4 ($E=109\text{GPa}$, and Poisson's ratio $\nu=0.34$) for its stable performance under high temperature. The impeller blade was subjected to a centrifugal force with the hub surface fixed. Thermal effect was neglected due to less impact

on the stress near the leading edge. [Figure 6](#) shows the stress contour of the blade. The maximum stress occurs at the hub of impeller exit which may be resulted from the excessively strong constraint.

Stress concentration occurs at the hub of the leading edge area. [Figure 7](#) shows the stress values along path 1 from left to right that is labeled in the red ellipse area of [Figure 6](#). The stress distribution at the hub of the impeller near the leading edge exhibits a single peak shape.

[Table 2](#) lists 8 different design conditions to ensure the universality of the strength prediction method. And the results of the FEM analysis were compared with those obtained by the strength prediction method. It can be seen that the strength prediction method shows good accuracy, the maximum errors are less than 3%.

3 Multidisciplinary optimization design of centrifugal compressor

3.1 Multidisciplinary optimization model

Combining the 1D aero-thermodynamic calculation and strength prediction method, the multidisciplinary design optimization method of centrifugal compressor during preliminary design stage was proposed. [Figure 8](#) shows the diagram of optimization procedure of centrifugal compressor. A centrifugal impeller with lowest pressure ratio of 4.4 was designed by means of this optimization method. At the beginning of optimization, the design variables initialization can be conducted based on the 1D aero-thermodynamic calculation. Then the initial design variable are simultaneously imported into aerodynamic analysis and mechanical analysis. Subsequently, the aerodynamic analysis results will be also imported to the mechanical analysis to calculate the maximum stress at impeller hub. And aerodynamic analysis and mechanical analysis are carried out in sequence. If the convergence is satisfied, the optimization process will stop. Otherwise, the calculated performance parameters in MDA system will be returned to the Isight optimizer and new design parameters will be evaluated.

The model of the centrifugal compressor optimization includes objective function, design variables and constraints. The design variables are shown in [Table 3](#). The

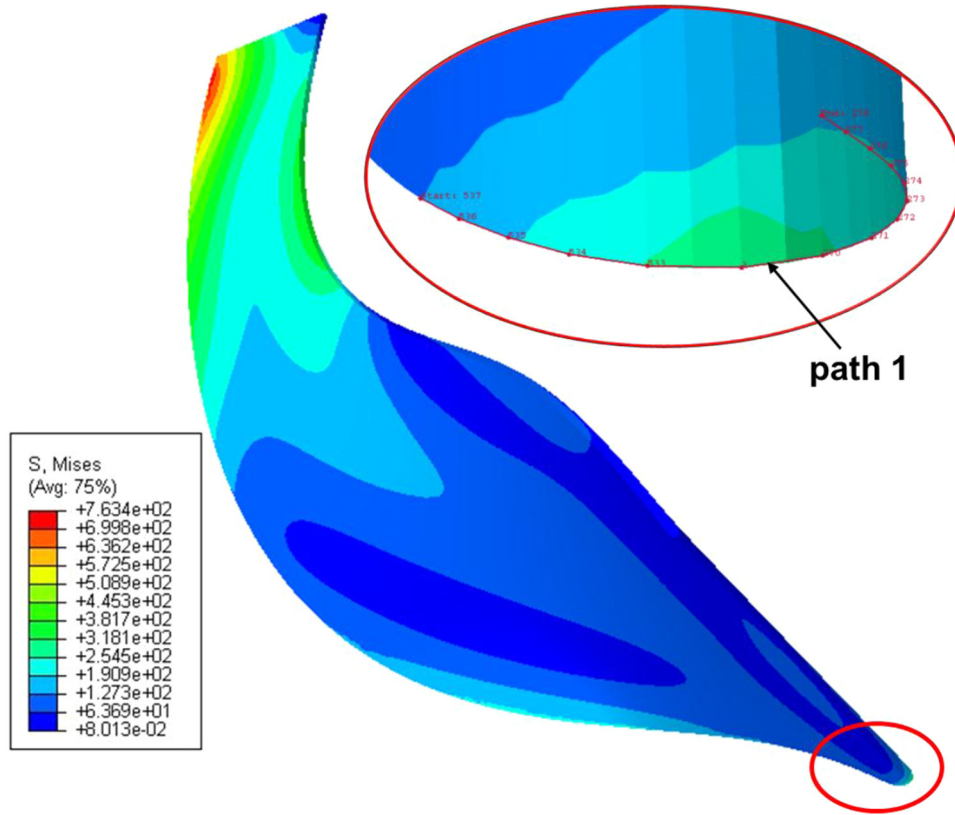


Fig. 6. Stress contour of the blade.

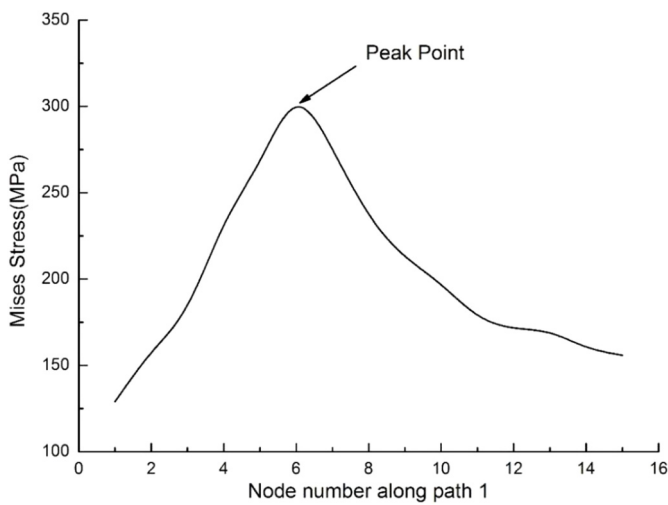


Fig. 7. Stress values along path 1.

variable bounds were determined based on the design experience in the literature that published in the past several decades. The given values of design parameters are obtained through the initial design results of 1D aero thermodynamic calculations.

In this paper, constraints of the preliminary optimization are set as follows:

- maximum stress at the hub near the leading edge σ ;
- pressure ratio of the centrifugal compressor π ;

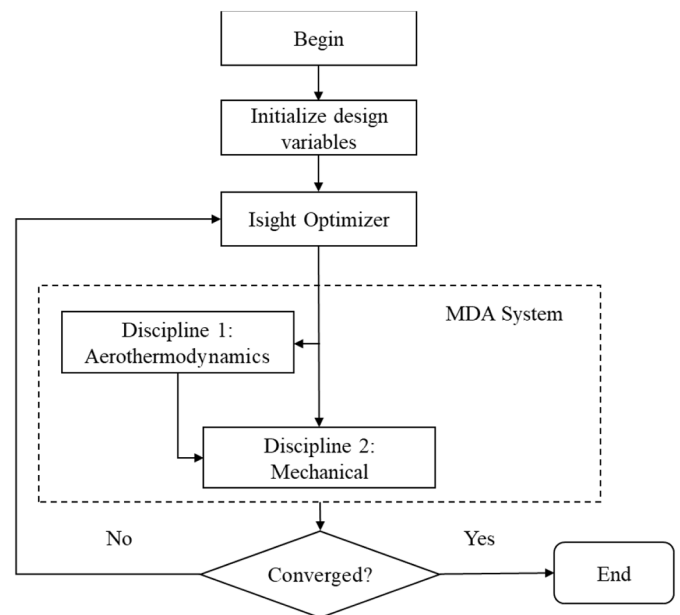


Fig. 8. Diagram of optimization procedure.

- the relative Mach number at the shroud of impeller inlet Ma_{1s} .

The details of the design constraints and the safety factors are shown in Table 4.

Table 3. Design variables of centrifugal compressor.

Parameters	Given values	Lower bounds	Upper bounds
r_{1h} (mm)	32.0	30.0	35.0
r_{1s} (mm)	91.34	85.0	98.0
r_2 (mm)	164.50	160.0	170.0
b_2 (mm)	22.90	20.0	25.0
L_Z (mm)	115.10	110.0	120.0
β_{1h} (°)	26.34	20.0	30.0
β_{1s} (°)	50.90	45.0	52.0
β_2 (°)	-30.00	-35.0	-25.0

Table 4. Constraints and safety factors of the centrifugal compressor.

Constrained parameters	Symbols of safety factors	Lower bounds	Upper bounds
PR	PR_{design}	4.4	–
σ	$[\sigma]$	–	650 (MPa)
Ma_{1s}	$[Ma_{1s}]$	–	1.2

The objective of the present optimization is to find the maximum efficiency with sufficient surge margin under the constraints of strength and aerodynamic requirements. The optimization can be expressed in a mathematic model as equation (9).

$$\begin{aligned} & \text{Maximize } \text{Eff}, SM \\ & \text{s.t. } \begin{cases} \sigma < [\sigma] \\ PR \geq PR_{\text{design}} \\ Ma_{1s} < [Ma_{1s}] \end{cases} \end{aligned} \quad (9)$$

3.2 Optimization results

The optimization was completed based on Isight commercial software using Non-dominated Sorting Genetic Algorithm-II (NSGA-II), which is excellent as a multi-object optimization method. Table 5 shows the parameters comparison between the optimal design and the original design. Optimal design 1 set the maximum of pressure ratio as the third optimization target rather than constraint. While Optimal design 2 were obtained following the optimization model of equation (9).

The results of optimal design 2 show that the efficiency of the impeller improves by 2.24%. And the impeller pressure ratio is slightly decreased. It can be seen that the maximum stress value at the impeller hub near the leading edge becomes larger, which is because of the increased inlet blade height. In addition, the surge margin of the

Table 5. Parameters comparison between the optimization design and the original design.

Parameter	Original design	Optimal design 1	Optimal design 2
r_{1h} (mm)	32.0	30.00	30.01
r_{1s} (mm)	91.34	93.56	97.99
r_2 (mm)	164.50	169.92	165.65
b_2 (mm)	22.90	21.80	20.94
L_Z (mm)	115.10	112.12	112.08
β_{1h} (°)	26.34	29.72	29.75
β_{1s} (°)	50.90	47.33	47.34
β_2 (°)	-30.00	-34.82	-34.99
η	86.261	87.923	88.506
SM	0.3273	0.3455	0.3727
PR	4.467	4.82	4.406
Ma_{1s}	1.05	0.912	0.821
σ (MPa)	287.529	307.13	339.273

impeller improves significantly. When the pressure ratio was set as the third optimization target, the optimized pressure ratio was up to 4.82. The impeller efficiency and surge margin decreased compared to Optimal design 2, however, the impeller efficiency and surge margin are still higher than the original design. It is noticed that the maximum stress value of optimal design 1 is less than that of optimal design 2, but larger than the original design. This is because of the difference of the inlet blade height. Besides, it can be inferred that the strength requirement will limit the development of high performance of centrifugal compressor with high aerodynamic efficiency and large surge margin. During the optimization process, 8 core CPU was used, and the overall time for optimization is about 20 minutes after 600 optimized iterations, which is very time-saving.

4 3D validation of optimal design

The blade modeling method is described in Section 2.3. The blade thickness at the shroud is normally designed as thin as practicable to get an optimum efficiency. Splitters are added to the impeller for high pressure ratio, and it is just a cut-back main blade.

4.1 3D validation of aerodynamic performance

The optimal design 1 was verified by a 3D CFD code Numeca, and S-A turbulence models was applied for its fine stability. For the near-wall grid, the y^+ of the mesh were less than 5 and the corresponding distribution is shown in Figure 9. The impeller flow field was using H&I mesh topology with about 3,100,000 grid nodes. The inlet total temperature 287.15 K, total pressure 1,01,325 Pa and axial flow direction were given as the compressor inlet boundary condition.

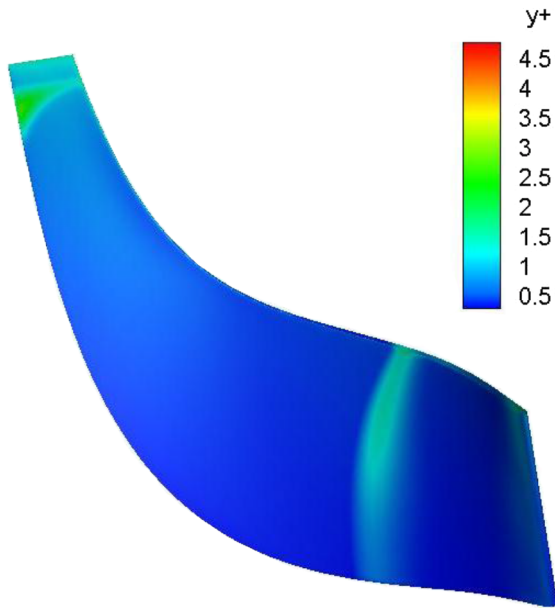


Fig. 9. y^+ distribution of the blade mesh.

Figure 10 presents contour plot of static pressure on the meridional plane of the impeller. The results show that the static pressure distributes smoothly through the impeller as expected. The aerodynamic performance results of the 3D aerodynamic calculation are listed in Table 6, which agree well with the results of Optimal design 1. The pressure ratio calculated by 3D CFD is higher than the preliminary results, which is mainly induced by the added splitter blades.

4.2 Strength check

In order to verify the structural strength accurately predicted by the preliminary design based on the multidisciplinary method, a 3D model of a sector of centrifugal impeller with a single blade was established. Considering the effects of pressure and temperature on the structural analysis, the aerodynamic results were involved in the strength check process. Thanks to the mesh difference between aerodynamic analysis and structural analysis, the inverse distance weighted (IDW) method was used as the interpolation method to transfer the physical information (pressure, temperature and mesh property, etc.) from aerodynamic analysis to mechanical analysis. A 3D IDW method can be formulated as:

$$F(x, y, z) = \frac{\sum_{i=1}^N w_i(x, y, z) f_i}{\sum_{i=1}^N w_i(x, y, z)} \quad (10)$$

where

$$w_i(x, y, z) = 1/d_i^\mu$$

$$d_i = \sqrt{(x - x_i)^2 + (y - y_i)^2 + (z - z_i)^2}.$$

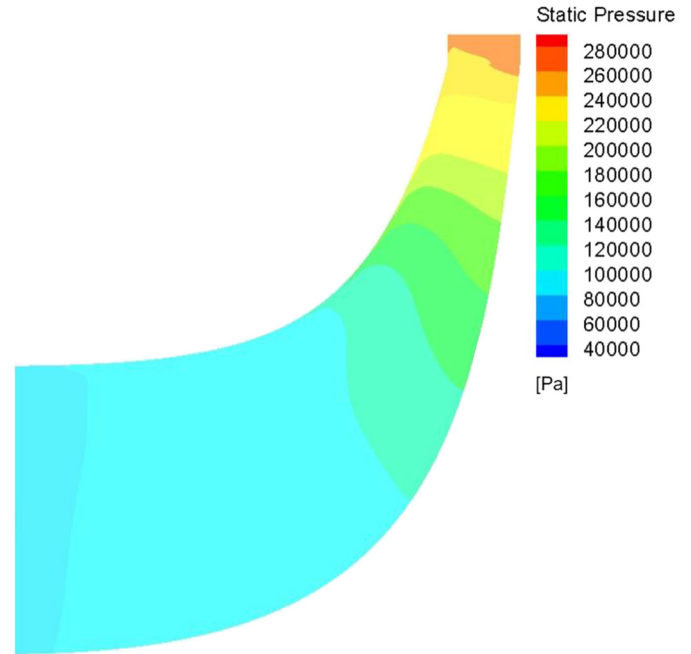


Fig. 10. Meridional view of static pressure through the impeller.

Table 6. Comparison between the results of 3D validation and Optimal design 1.

	3D validation	Optimal design 1
η (%)	89.48	87.923
SM	0.3291	0.3455
PR	5.255	4.82

The information of pressure field and temperature field obtained by NUMECA was interpolated into the structural computational nodes using IDW method. Figure 11 shows the temperature distribution on blade surface calculated by NUMECA and the interpolation results, which exhibits good agreement.

The mechanical analysis was conducted using ABAQUS. The calculated stress distribution of the impeller is as shown in Figure 12, and the maximum stress of the impeller hub near the leading edge is 313.082MPa, which is nearly equal to the predicted results of Optimal design 1. Besides, it can be seen that the maximum stress occurs at the center of the impeller, which is resulted from the large centrifugal force at impeller outlet area.

5 Conclusions

This paper presents a preliminary design method by considering multidisciplinary coupling. An 1D strength prediction method was proposed to evaluate the maximum stress at the impeller hub near the leading edge. The multidisciplinary design optimization system of preliminary

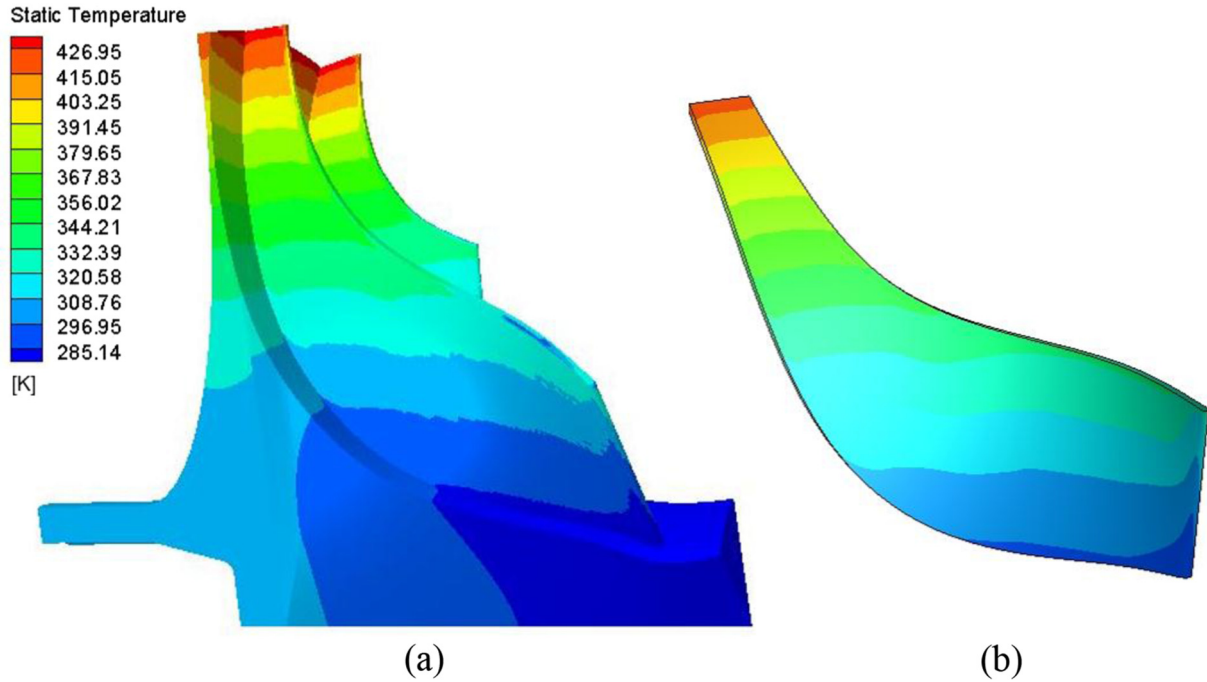


Fig. 11. Temperature distribution of centrifugal impeller blade (a) after interpolation; and (b) before interpolation.

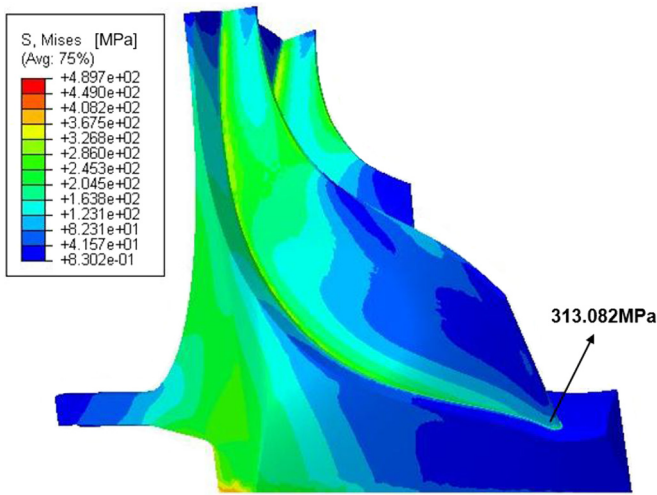


Fig. 12. Stress distribution of compressor impeller.

design was established and used to design a centrifugal compressor with a lowest pressure ratio of 4.4. The conclusions of the study are as follows:

- An equivalent strength prediction model was established to simulate the stress state of impeller hub near the leading edge area. The strength prediction formulation was deduced by considering tensile stress induced by centrifugal force and moment induced by blade twist, aerodynamic force and thermal effect. Then the 1D strength method was verified by 3D finite element data, and the maximum errors were less than 3%.

- The preliminary design of a centrifugal compressor with lowest pressure ratio of 4.4 is executed based on multidisciplinary design optimization method. The results show that the structural strength is closely related to the blade inlet height. The maximum aerodynamic efficiency of the optimized impeller is 88.506% with pressure ratio of 4.406. Another optimal design with higher pressure ratio up to 4.82 sacrifices aerodynamic efficiency and surge margin.
- The 3D CFD was applied to analyze the aerodynamic performance of the optimized centrifugal compressor. The calculated results agreed well with the preliminary design results. The efficiency was up to 89.48% with a pressure ratio of 5.255. The higher pressure ratio was produced by the added splitter blades. Besides, the complete mechanical analysis of centrifugal impeller was carried out, the maximum stress at the impeller hub near the leading edge was 313.082MPa, which was consistent with the strength prediction results.

Nomenclature

P	Pressure
T	Temperature
k	Ratio of specific heats
R	Gas constant
η	Efficiency
U	Impeller blade tip speed
C	Absolute gas velocity
W	Relative gas velocity
α	Absolute air angle

β	Relative air angle
Δh	Enthalpy change (J/kg)
μ	Slip factor
Z	Blade number
D_f	Diffuser factor
D	Diameter
L_B	Impeller flow length
C_f	Skin friction coefficient
D_{hyd}	Impeller average hydraulic diameter
L_z	Axial length of impeller
b	Blade height
r	Radius
Δn_{cl}	Clearance
ρ	Density
$\varepsilon_{\text{wake}}$	Wake fraction of blade-to-blade space
\dot{m}	Mass flowrate
Re	Reynolds number
ν	Kinematic viscosity
ΔV	Volume of blade element
t	Blade thickness
PR	Stage total-to-total pressure ratio
M_a	Mach number
SM	Surge margin
σ	Max stress of impeller blade

Subscripts

0	Total condition
1	Impeller inlet
2	Impeller exit
l	Impeller
m	Meridional direction
θ	Tangential direction
s	Shroud
h	Hub
d	Diffuser passage length

Acknowledgements. National Science and Technology Major Project (2017-II-0006-0019) and National Natural Science Foundation of China (11902259) support this work.

References

- [1] P.Y. Li, C.W. Gu, Y. Song, A new optimization method for centrifugal compressors based on 1d calculations and analyses. *Energies* **8**, 4317–4334 (2015)
- [2] K.V. Muralidharan, Design of a Centrifugal Compressor Using CFD Analysis Part I Preliminary Design and Geometry Modification, Proceedings of the Asme International Mechanical Engineering Congress and Exposition, 2014, Vol. 1, 2015
- [3] A. Whitfield, Preliminary design and performance prediction techniques for centrifugal compressors, *Proc. Inst. Mech. Eng. A* **204**, 131–144 (1990)
- [4] S. Yoon, J.H. Baek, A sensitivity analysis of centrifugal compressors' empirical models, *KSME Int. J.* **15**, 1292–1301 (2001)
- [5] H.W. Oh, E.S. Yoon, M.K. Chung, An optimum set of loss models for performance prediction of centrifugal compressors, *Proc. Inst. Mech. Eng. A* **211**, 331–338 (1997)
- [6] M.R. Galvas, FORTRAN program for predicting off-design performance of centrifugal compressors. *Work*, 1973
- [7] R.H. Aungier, Mean streamline aerodynamic performance analysis of centrifugal compressors, *J. Turbomach.* **117**, 360–366 (1995)
- [8] A.H. Zahed, N.N. Baymi, Design procedure of centrifugal compressors, *ISESCO J. Sci. Technol.* **10**, 14 (2014)
- [9] C. Xu, Centrifugal compressor design considerations, *Proc. ASME Fluids Eng. Div. Summer Conf.* **2**, 217–225 (2006)
- [10] A.H. Lerche, J.J. Moore, N.M. White, J. Hardin, in *ASME Turbo Expo 2012: Turbine Technical Conference and Exposition*, 2012, 191–200
- [11] H.S. Kang, Y.J. Kim, Optimal design of impeller for centrifugal compressor under the influence of one-way fluid-structure interaction, *J. Mech. Sci. Technol.* **30**, 3953–3959 (2016)
- [12] AIAA, Evaluation of multidisciplinary optimization approaches for aircraft conceptual design, *AIAA J* (2004)
- [13] Y.U. Ming, Centrifugal compressor design system based on multidisciplinary design optimization, *J. Mech. Streng.* (2012)
- [14] Y.S. Zhang, B. Zhao, Y.S. Liu, Z.F. Yue, Reliability-based multidisciplinary design optimization for centrifugal compressor using the fourth moment method, *Adv. Mater. Res.* **156–157**, 575–581 (2010)
- [15] P.M. Came, C.J. Robinson, Centrifugal compressor design, *Proc. Inst. Mech. Eng. C* **213**, 139–155 (1999)
- [16] J.D. Stanitz, One-dimensional compressible flow in vaneless diffusers of radial- and mixed-flow centrifugal compressors, including effects of friction, heat transfer and area change, Technical Report Archive & Image Library, 1952
- [17] F.J. Wiesner, A review of slip factors for centrifugal impellers, *J. Eng. Gas Turbines Power* **89**, 558 (1967)
- [18] X. Qiu, D. Japikse, J. Zhao, M.R. Anderson, in *ASME Turbo Expo 2010: Power for Land, Sea, and Air*, 2011, pp. 1711–1721
- [19] G. Ferrara, L. Ferrari, C.P. Mengoni, M. De Lucia, L. Baldassarre, Experimental investigation and characterization of the rotating stall in a high pressure centrifugal compressor: Part I — influence of diffuser geometry on stall inception, Proceedings of the ASME Turbo Expo 2002: Power for Land, Sea, and Air. Volume 5: Turbo Expo 2002, Parts A and B. Amsterdam, The Netherlands, June 3–6, 2002, pp. 613–620
- [20] G. Ferrara, L. Ferrari, C.P. Mengoni, M. De Lucia, L. Baldassarre, Experimental investigation and characterization of the rotating stall in a high pressure centrifugal compressor: Part II — Influence of diffuser geometry on stage performance, Proceedings of the ASME Turbo Expo 2002: Power for Land, Sea, and Air. Volume 5: Turbo Expo 2002, Parts A and B. Amsterdam, The Netherlands, 2002, 621–628
- [21] A. Whitfield, N.C. Baines, Design of Radial Turbomachines. Longman Scientific & Technical, 1990
- [22] J.D. Denton, Loss mechanisms in turbomachines, *J. Turbomach.* **115**, V002T014A001 (1993)
- [23] J.E. Coppage, F. Dallenbach, Study of supersonic radial compressors for refrigeration and pressurization systems, *Inf. Process. Lett.* **1**, 157–163 (1956)

- [24] W. Jansen, A method for calculating the flow in a centrifugal impeller when entropy gradients are present, Royal Society Conference on Internal Aerodynamics (Turbomachinery), 1967, pp. 133–146
- [25] J.P. Johnston, J.R.C. Dean, Losses in vaneless diffusers of centrifugal compressors and pumps: analysis, experiment, and design, *J. Eng. Power* **88**, 49–60 (1966)
- [26] J.W. Daily, R.E. Nece, Chamber dimension effects on induced flow and frictional resistance of enclosed rotating disks, *J. Basic Eng. Trans. ASME* **82**, 217–230 (1960)
- [27] D. Japikse, paper presented at the IME Conference on Turbocharging and Turbochargers, 1982
- [28] A. Ceruti, V. Voloshin, P. Marzocca, Heuristic algorithms applied to multidisciplinary design optimization of unconventional airship configuration, *J. Aircraft* **51**, 1758–1772 (2014)
- [29] S.P. Wen, J. Wang, T. Li, G. Xi, Reducing solid particle erosion of an axial fan with sweep and lean using multidisciplinary design optimization. *Proc. Inst. Mech. Eng. C* **228**, 2584–2603 (2014)
- [30] D.B. Meng, H.Z. Huang, Z.L. Wang, N.C. Xiao, X.L. Zhang, Mean-value first-order saddlepoint approximation based collaborative optimization for multidisciplinary problems under aleatory uncertainty, *J. Mech. Sci. Technol.* **28**, 3925–3935 (2014)

Cite this article as: S. Shouyi, Y. Zhufeng, L. Lei, Z. Mengchuang, Y. Weizhu, Preliminary design of centrifugal compressor using multidisciplinary optimization method, *Mechanics & Industry* **20**, 628 (2019)